Oxidative stress generated by hemorrhagic shock recruits Toll-like receptor 4 to the plasma membrane in macrophages

Kinga A. Powers, Katalin Szászi, Rachel G. Khadaroo, Patrick S. Tawadros, John C. Marshall, András Kapus, and Ori D. Rotstein

Departments of Surgery, St. Michael's Hospital and University Health Network, and Department of Surgery, University of Toronto, Toronto, Ontario, M5G 2C1, Canada

Oxidative stress generated by ischemia/reperfusion is known to prime inflammatory cells for increased responsiveness to subsequent stimuli, such as lipopolysaccharide (LPS). The mechanism(s) underlying this effect remains poorly elucidated. These studies show that alveolar macrophages recovered from rodents subjected to hemorrhagic shock/resuscitation expressed increased surface levels of Toll-like receptor 4 (TLR4), an effect inhibited by adding the antioxidant *N*-acetylcysteine to the resuscitation fluid. Consistent with a role for oxidative stress in this effect, in vitro H_2O_2 treatment of RAW 264.7 macrophages similarly caused an increase in surface TLR4. The H_2O_2–induced increase in surface TLR4 was prevented by depleting intracellular calcium or disrupting the cytoskeleton, suggesting the involvement of receptor exocytosis. Further, fluorescent resonance energy transfer between TLR4 and the raft marker GM1 as well as biochemical analysis of the raft components demonstrated that oxidative stress redistributes TLR4 to lipid rafts in the plasma membrane. Preventing the oxidant-induced movement of TLR4 to lipid rafts using methyl-β-cyclodextrin precluded the increased responsiveness of cells to LPS after H_2O_2 treatment. Collectively, these studies suggest a novel mechanism whereby oxidative stress might prime the responsiveness of cells of the innate immune system.

CORRESPONDENCE
Ori D. Rotstein:
rotsteino@smh.toronto.on.ca

Abbreviations used: AM, alveolar macrophage; BAPTA/AM, 1,2-bis-(2-aminophenoxy)-ethane-N,N,N',N'-tetraacetic acid tetra(acetoxymethyl) ester; CT_xB, cholera toxin B; FRET, fluorescent resonance energy transfer; MβCD, methyl-β-cyclodextrin; MyD88, myeloid differentiation primary response gene 88; NAC, *N*-acetylcysteine; S/R, shock/resuscitation; TLR4, Toll-like receptor 4.

Acute respiratory distress syndrome after resuscitated hemorrhagic shock in trauma patients is an important contributor to late morbidity and mortality (1, 2). It has been suggested that shock/resuscitation (S/R) promotes organ injury by priming cells of the innate immune system for excessive responsiveness to a subsequent proinflammatory stimulus (3, 4). Several groups, including our own, have modeled this "two-hit" phenomenon both in vivo and in vitro to gain insight into the pathophysiological mechanisms underlying the priming events. Our previous work has defined a central role for activated alveolar macrophages (AMs) in augmented lung injury after S/R. AMs recovered from resuscitated animals exhibited exaggerated LPS responsiveness with excessive generation of proinflammatory molecules, including cytokine-induced neutrophil chemoattractant, the rodent ortholog of IL-8, and TNF-α (5, 6). Increased expression of these proteins was due to enhanced gene transcription, a result of earlier and heightened nuclear translocation of the transcription factor NF-κB in response to LPS. Further, oxidative stress during ischemia/reperfusion appeared to be responsible for this priming phenomenon, as inclusion of the antioxidant *N*-acetylcysteine (NAC) in the resuscitation fluid prevented the increased responsiveness to LPS. To date, the mechanisms responsible for the ability of oxidative stress to prime for increased LPS responsiveness are not fully elucidated.

One potential mechanism of S/R-induced priming for enhanced inflammatory response is through potentiation of various components of LPS-induced signaling. Several intracellular pathways whereby LPS stimulation leads to dissociation of NF-κB from the cytosolic IκB/NF-κB complex and translocation of NF-κB into the nucleus have been described. Recent studies have identified the Toll-like receptor 4 (TLR4) as the main upstream sensor for LPS both in vitro and in vivo. Optimal activation of the TLR4 signaling pathway by LPS involves the formation of an LPS signaling complex consisting of surface molecules, such as CD14 and MD2, as well as intracellular adaptor molecules,

including myeloid differentiation primary response gene 88 (MyD88) and IRAK (7). Recently, several factors have been identified that contribute to the responsiveness of TLR4. These include receptor dimerization, mobilization to lipid rafts, and formation of a TLR4 activation cluster including other proteins, such as heat shock proteins 70 and 90, chemokine receptor 4, and growth differentiation factor 5 (8, 9). The total number of functional TLR4 molecules expressed on the cell surface may also influence LPS response. Cells lacking TLR4 or expressing a mutant receptor exhibit marked hyporesponsiveness to LPS (10), and overexpression of surface TLR4 was shown to augment LPS responsiveness (11, 12). Collectively, these observations imply that physiological/pathophysiological alterations in the expression of surface TLR4 in vivo may be one mode of influencing LPS responsiveness. In this regard, Nomura et al. (13) reported that induction of LPS tolerance in peritoneal macrophages correlated with the ability of LPS to down-regulate surface TLR4. We have previously reported that S/R prevented the LPS-induced reduction in TLR4 protein and mRNA levels in whole lung tissue (14). However, TLR4 levels did not exceed baseline in shock plus LPS-treated animals, making it unlikely that total cellular TLR4 per se influenced LPS reactivity. These observations raised the hypothesis that S/R might alter cellular distribution of the TLR4 receptor complex as a mechanism underlying increased responsiveness to LPS.

In these studies, we demonstrate that S/R causes translocation of TLR4 in AMs from the cytoplasm to the plasma membrane, thus elevating TLR4 surface expression. The central role of oxidative stress in this process was shown by the ability of NAC to prevent this translocation in vivo and by the ability of exogenously added H_2O_2 to recapitulate the translocation in RAW 264.7 cells in vitro. We also show that TLR4 is mobilized into lipid rafts and that this is essential for oxidant-induced translocation. Finally, the ability of oxidative stress to induce the formation of a surface TLR4 receptor complex within lipid rafts contributed to the augmented responsiveness to LPS. Collectively, these findings suggest a novel mechanism whereby oxidative stress generated during S/R, a form of global ischemia/reperfusion, might prime the innate immune system for an exaggerated response to inflammatory stimuli and hence for increased tissue and organ injury.

RESULTS

Resuscitated shock induces cell surface TLR4 expression in AMs

To determine the effect of resuscitated hemorrhagic shock on TLR4 distribution, we isolated AMs from sham and S/R rats. At the end of resuscitation, total cell numbers obtained by bronchoalveolar lavage and percentage of macrophages (>90%) did not differ from sham animals (5). Phase microscopy shows that AMs from sham and S/R animals exhibited similar morphology (Fig. 1 A). Immunofluorescence staining of permeabilized cells revealed that in sham cells, TLR4 was distributed throughout the cytoplasm. In contrast, in cells from S/R animals, there was peripheralization of TLR4 with diminished cytoplasmic staining. This phenomenon was observed in 58.2 ± 4.1% of cells from S/R animals compared with <20% in sham groups (Fig. 1 B). The redistribution of TLR4 to the periphery in S/R cells was confirmed by confocal microscopy (Fig. 1 C, compare top row with middle row). To confirm specificity of the TLR4 antibodies used in our studies, we performed immunostaining on macrophages from C57BL10/ScCr animals, known to be null for TLR4 expression. No fluorescence was observed in these cells (not depicted). In addition, on Western blot the H-80 antibody reacted with a protein at the appropriate molecular mass of TLR4 (not depicted). Fig. 1 E demonstrates that the observed immunofluorescence staining pattern was indeed due to binding of the TLR4 antibody.

To determine TLR4 surface expression, TLR4 staining of nonpermeabilized cells was quantified using flow cytometry. In a representative study (Fig. 2 A), there was a marked increase in cell surface TLR4 in cells from S/R animals compared with sham. Over several studies, TLR4 surface level in S/R cells was significantly elevated (Fig. 2 B). Collectively, these findings demonstrate that S/R induces redistribution of

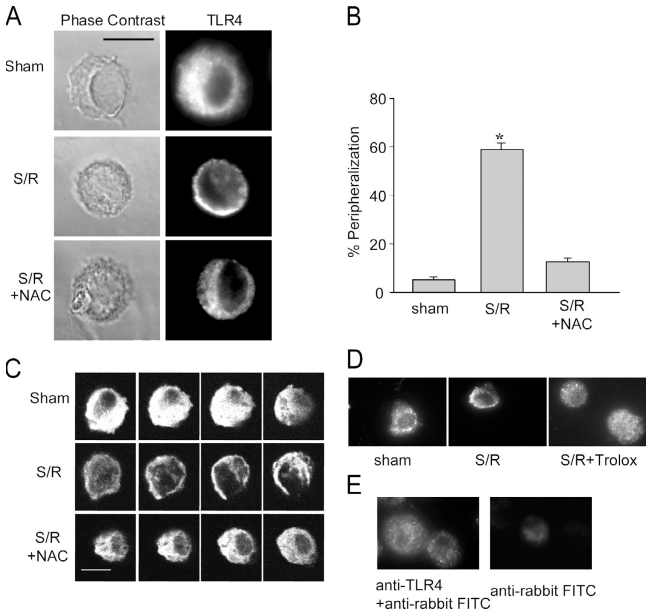

Figure 1. Redistribution of TLR4 in AMs after resuscitated hemorrhagic shock. AMs were isolated from sham animals or from animals that underwent hemorrhagic shock followed by resuscitation for 1 h (S/R). Where indicated, 0.5 g/kg NAC or 10 mg/kg Trolox was present during resuscitation (S/R+NAC, S/R+Trolox, respectively). Cells were allowed to adhere to coverslips, fixed, permeabilized, and stained with anti-TLR4. (A and D) Typical phase contrast and fluorescence microscopy images are shown. (B) Peripheralization of TLR4 was quantified by Scionimage software as described in Materials and methods. (C) Pictures in rows show confocal microscopic images of different focal planes of the same cell. Bars, 10 μm. (E) Specificity of the TLR4 antibody. Staining was performed with (left) or without (right) anti-TLR4. Both samples were stained with FITC-labeled secondary antibody.

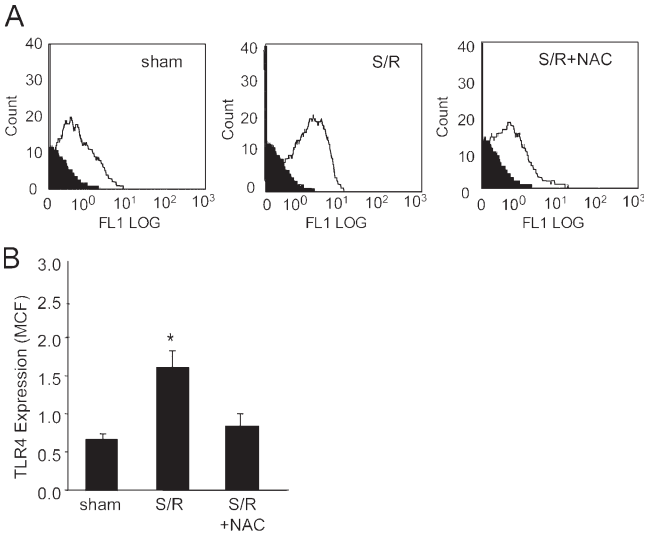

Figure 2. Resuscitated hemorrhagic shock increases TLR4 surface levels. AMs were stained live with anti-TLR4 and FITC-conjugated secondary antibody. Fluorescence was analyzed by flow cytometry as described in Materials and methods. (A) Profiles of fluorescence intensity of TLR4 staining (black line) or controls (secondary antibody only, solid). (B) Changes in TLR4 surface expression (mean channel fluorescence [MCF]) after the indicated treatments. Data are mean ± SEM. $n = 4$ animals per group. *, $P < 0.05$ for S/R versus all other groups.

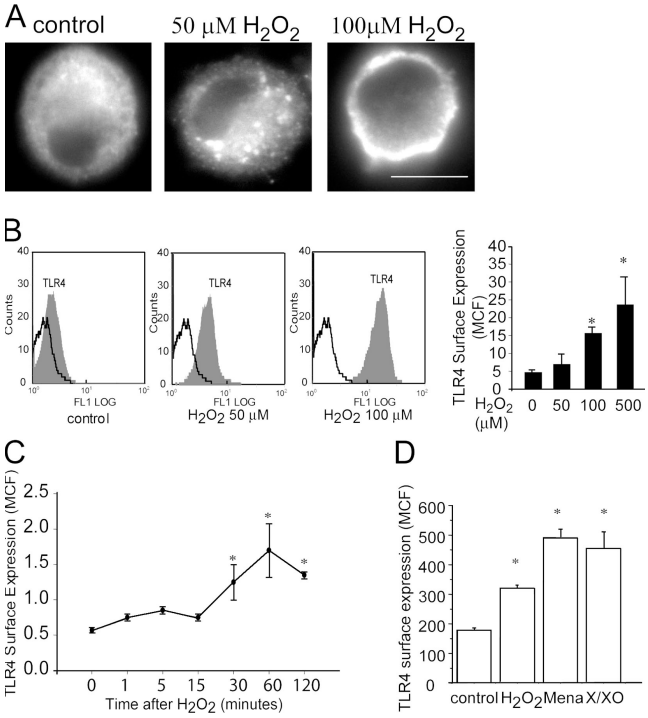

Figure 3. Oxidative stress induces increased TLR4 surface expression in RAW 264.7 cells. (A) RAW 264.7 cells, exposed to H_2O_2 for 1 h, were stained with anti-TLR4/MD2-FITC antibody. Representative fluorescence microscopy images ($n = 4$). (B and C) Dose and time dependence of the H_2O_2 effect. Cells were treated with the indicated concentration of H_2O_2 for 1 h (B) or with 100 μM H_2O_2 for the indicated time (C). TLR4 staining was analyzed using flow cytometry. In B, representative profiles of fluorescence intensity of TLR4 staining (gray solid) or unstained controls (black line) are shown (left panels). (D) RAW cells were treated with 50 μM menadione (Mena) or 100 μM H_2O_2 or 0.1 mM xanthine and 3 U/ml xanthine oxidase for 1 h. Surface TLR4 was measured as in B. The graphs show mean ± SEM of $n = 3$ (for D) or 4 (for B and C). *, $P < 0.05$ for points indicated versus control.

TLR4 from the cytoplasmic compartment to the periphery, including onto the plasma membrane. Previous work from several groups suggests that oxidative stress generated during reperfusion of the gastrointestinal tract contributes to distant cellular priming and activation. NAC supplementation in the resuscitation fluid prevented both the S/R-induced increase of isoprostanes in the blood (a marker of oxidative stress) and priming of AMs (5, 15). To test the role of oxidants in the S/R-induced TLR4 redistribution, we added NAC to the resuscitation fluid. NAC blocked both the redistribution of TLR4 after S/R (Fig. 1, A and C, bottom, and B, right bar) and the increase in TLR4 cell surface expression (Fig. 2, A and B). To further substantiate the role of oxidative stress, we tested the effect of Trolox, a water-soluble vitamin E analogue that is a well-established antioxidant agent. Similar to NAC, Trolox added to the resuscitation fluid prevented the redistribution of TLR4 in AMs (Fig. 1 D). In addition, Trolox impaired lung neutrophil sequestration to the same extent as NAC (not depicted). We next asked whether exposure of cells to oxidants could mimic the effect of S/R on TLR4 distribution. Fig. 3 A demonstrates that a 1-h treatment of RAW 264.7 cells with 100 μM H_2O_2 induces peripheralization of TLR4 in a pattern reminiscent of that observed in bronchoalveolar lavage cells after S/R. Treatment with 50 μM H_2O_2 appeared to accentuate a vesicular pattern of TLR4 distribution. By flow cytometry, H_2O_2 was shown to induce a dose-dependent increase in surface expression of TLR4, with modest effect at 50 μM and marked increase at 100–500 μM (Fig. 3 B, representative study shown in the left panels). Concentrations of H_2O_2 up to 200 μM did not induce cell death as determined by trypan blue exclusion, whereas 500 μM caused ~50% cell death (not depicted). Quantitation of several studies confirmed the dose dependency (Fig. 3 B, right panel). A time course shows that 100 μM H_2O_2 induces a progressive increase in cell surface TLR4 starting as early as 1–5 min and peaking at 30–120 min (Fig. 3 C). We also tested the effect of alternative agents known to induce oxidative stress. Menadione accumulates in the cells and induces intracellular oxidative stress, whereas the xanthine/xanthine oxidase system is able to produce extracellular oxidants. Both agents caused a marked increase in TLR4 expression in the cell surface as shown by flow cytometry (Fig. 3 D). In aggregate, these findings are consistent with a role for oxidative stress in the increased surface expression of TLR4 after S/R. In subsequent studies, a dose of 100 μM H_2O_2 for 1 h will be studied. This protocol corresponds to conditions used in our previous studies showing that H_2O_2 primes RAW 264.7 cells for increased responsiveness to LPS (16, 17).

Effect of resuscitated hemorrhagic shock on localization of TLR4 to lipid rafts

Lipid rafts are considered to be important contributors to membrane recruitment and clustering of signaling molecules (18). Recent studies have reported that clustering of the LPS receptor complex upon LPS stimulation required lipid rafts (19–22). Therefore, we next evaluated the role of lipid rafts in the oxidative stress–induced TLR4 redistribution.

AMs from S/R animals were stained live using rhodamine–cholera toxin B (CT_xB), and then fixed, permeabilized, and stained for TLR4. As shown in Fig. 4 A, AMs from sham animals displayed diffuse intracellular TLR4 staining, whereas GM1 ganglioside, a classical raft marker was mainly localized to the cell surface with minimal colocalization with TLR4. In contrast, TLR4 in cells from S/R animals displayed a peripheral staining (55 ± 2.3%, $n = 3$; Fig. 4 A, bottom row), and it colocalized with GM1 as shown by the overlay image. Supporting the critical role of oxidants in the effect, NAC added in the resuscitation fluid prevented TLR4 redistribution and its colocalization with GM1 (7.5 ± 0.5%, $n = 3$; Fig. 4 A, right).

The effect of oxidant stress on localization of TLR4 in lipid rafts was also examined in vitro by exposing RAW 264.7 cells to H_2O_2. Fig. 4 B illustrates that H_2O_2 induces colocalization of TLR4 with GM1 in the plasma membrane. We used methyl-β-cyclodextrin (MβCD) to deplete cellular cholesterol and disrupt lipid rafts (23) before adding H_2O_2 to RAW 264.7 cells. This treatment prevented movement of TLR4 to the cell surface (Fig. 4 B, right). The inhibitory effect of cholesterol depletion was also confirmed by flow cytometry. Live cells treated with MβCD either before or after H_2O_2 were stained with anti-TLR4/MD2. As shown in Fig. 4 C, when applied before H_2O_2 treatment, MβCD prevented the oxidant-induced TLR4 surface up-regulation. However, when oxidant exposure was performed before raft disruption with MβCD, increased TLR4 levels persisted on the cell surface (Fig. 4 C). MβCD may exert its effect through altering cellular responsiveness to H_2O_2. To examine this possibility, we tested the effect of H_2O_2 on p38 in MβCD-treated cells. As shown in Fig. 4 D, cholesterol depletion did not prevent H_2O_2-induced phosphorylation of p38. Although we cannot rule out that cholesterol depletion might interfere with some pathways, these data show that MβCD does not exert a global inhibition of oxidant-induced signaling.

To substantiate lipid raft localization of TLR4, we isolated raft fractions using discontinuous sucrose gradient ultracentrifugation of RAW264.7 cells (24). Effective isolation of membrane rafts was confirmed by the presence of GM1

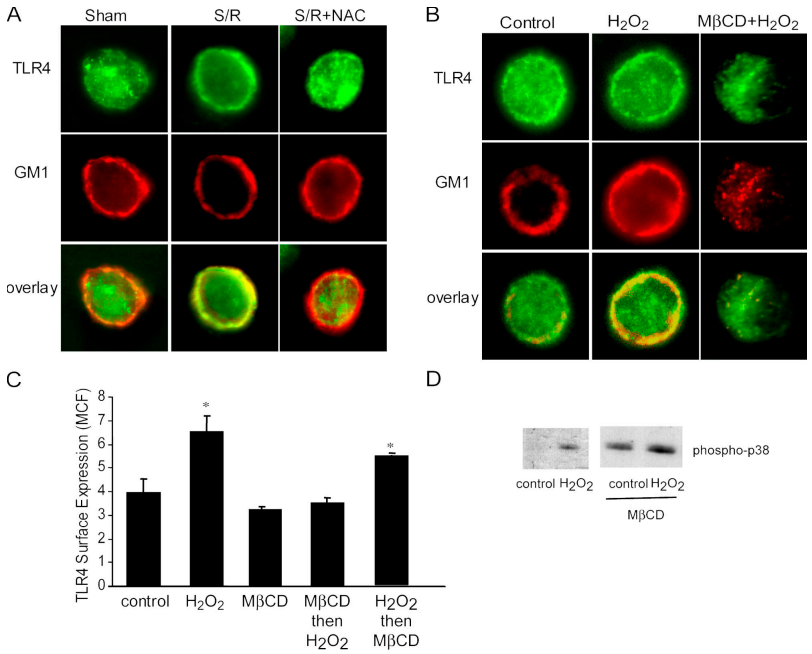

Figure 4. Oxidant stress induces clustering of TLR4 in plasma membrane lipid rafts. (A). TLR4 and GM1 colocalization after oxidant stress. AMs were plated on coverslips and stained live at 4°C with rhodamine-CT_xB. The cells were then fixed, permeabilized, and stained with anti-TLR4. Representative images are shown of TLR4 (green), rhodamine-CT_xB staining (red), or the merged image. (B) RAW 264.7 cells were treated with 100 μM H_2O_2 for1 h. Where indicated, cells were depleted from cholesterol by incubating with 10 mM MβCD for 30 min before H_2O_2. Cells were stained and visualized as in A. (C) H_2O_2-induced increase in TLR4 surface level requires lipid rafts. RAW264.7 cells were treated with 100 μM H_2O_2 for 1 h. Where indicated, cells were depleted from cholesterol before or after treatment with H_2O_2. TLR4 expression was analyzed by flow cytometry. Data are mean ± SEM ($n = 4$ per group). *, $P < 0.05$ for H_2O_2, H_2O_2 then MβCD versus control and MβCD then H_2O_2. (D) Cholesterol depletion does not interfere with H_2O_2-induced signaling. Cells were treated with 100 μM H_2O_2 for 30 min and lysed. An equal amount of protein was loaded on SDS gels, and phospho-p38 was detected using Western blotting. Where indicated, cells were cholesterol depleted before H_2O_2 addition.

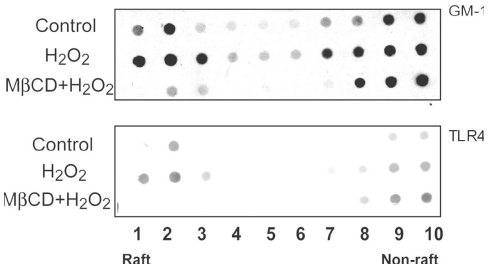

Figure 5. Recruitment of TLR4 into lipid rafts by oxidant stress. RAW 264.7 cells, treated with 100 μM H_2O_2 for 1 h with or without MβCD pretreatment, were lysed in 1% Triton X-100 and subjected to discontinuous sucrose density gradient centrifugation as described in Materials and methods. Fractions were analyzed by dot blotting using either CT_xB conjugated to horseradish peroxidase (GM1, top) or anti-TLR4 primary and peroxidase-coupled secondary antibody (bottom). Fractions 1–3 correspond to lipid rafts. Representative blots of three separate experiments are shown.

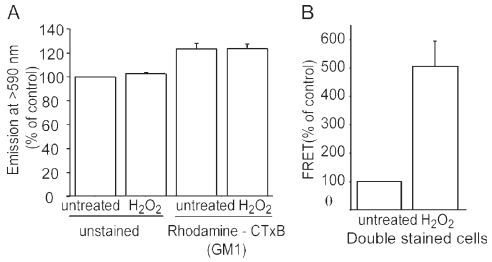

Figure 6. FRET verifies oxidant-induced molecular interaction between TLR4 and GM1. (A) Controls for FRET. Untreated or H_2O_2-treated (100 μM for 1 h) RAW 264.7 cells were either left unstained or stained live at 4°C with rhodamine-CT_xB. Fluorescence of individual cells was determined using the excitation wavelength 480 ± 5 nm and emission was ≥590 nm as described in Materials and methods. The emission of all groups was normalized to the unstained untreated cells (100%). Data are mean ± SEM of $n = 18$ cells from three independent experiments. (B) H_2O_2 induces FRET between rhodamine-CT_xB (GM1) and anti-TLR4-FITC. RAW 264.7 cells were left untreated or treated with 100 μM H_2O_2 for 1 h and stained live at 4°C with rhodamine-CT_xB, anti-TLR4, and FITC-labeled secondary antibody. For control, identically treated cells were stained only with FITC-labeled secondary antibody. To obtain the value of FRET, non-FRET–related factors were corrected for as detailed in Results. Data are normalized to the untreated cells (100%) and are mean ± SEM of $n = 24$ cells, $n = 4$.

ganglioside in the nonsoluble portion, fractions 1–3 of the sucrose gradient (Fig. 5, top). H_2O_2 stimulation induced localization of TLR4 to raft fractions (Fig. 5, bottom). This effect was prevented by pretreatment with MβCD.

Fluorescent resonance energy transfer (FRET) analysis was applied to examine the spatial proximity of TLR4 to GM1 ganglioside in lipid rafts. TLR4 was labeled using anti-TLR4 primary and an FITC-coupled Fab fragment secondary antibody, and GM1-ganglioside was stained with a rhodamine-coupled CT_xB. In the first series of experiments, we validated the system and determined how much of the fluorescence was due to other non-FRET–related factors to correct for them. We considered two potential problems. First, the excitation light used in these experiments (480 ± 5 nm) might also excite rhodamine and thus give a falsely high quantitation of FRET. To test this possibility, we stained cells with rhodamine-CT_xB only and measured emission at >590 nm after exciting with 480 ± 5 nm light (settings used for FRET). Fig. 6 A shows that H_2O_2 treatment did not alter the background fluorescence of unstained cells. Emission in the rhodamine-stained cells increased by 23 ± 4% compared with unstained cells. However, this increase was identical in the untreated and H_2O_2-treated cells. This verifies that H_2O_2 treatment does not interfere with the fluorescent measurements. To account for the fluorescence resulting from rhodamine excitation by the 480 ± 5 nm wavelength, the emission measured in double-stained cells during the FRET experiments was corrected by 23%. Second, we investigated whether part of the fluorescence detected at ≥590 nm could originate from residual FITC emission at the rhodamine emission wavelength. Indeed, control experiments revealed a linear correlation between green fluorescence intensity and the resulting bleed through emission detected at ≥590 nm (not depicted). Because H_2O_2 treatment increases TLR4 surface expression, the bleed through can be different in untreated and treated cells. Therefore, we carefully compensated for any bleed through of FITC into the emission wavelength used for FRET. The fluorescence of similarly treated single- (FITC only) and double- (FITC and rhodamine) stained cells was determined for each experiment under identical conditions. To obtain the value of real FRET, we first corrected the fluorescence of the double-stained cells by 23% (to compensate for the emission of rhodamine excited by the 480 ± 5 nm light; see above). The difference between the corrected fluorescence of the double-stained cells and the fluorescence measured in single-stained cells (i.e., the bleed through of FITC emission into ≥590 nm) is therefore attributed to the FRET between FITC-labeled anti-TLR4 and rhodamine-labeled GM1. Fig. 6 B illustrates that H_2O_2 treatment caused an approximately fivefold increase in FRET emission. This result is consistent with the conclusion that treatment with H_2O_2 induced molecular proximity of TLR4 with the raft marker GM1 ganglioside. Collectively, these results provide evidence that oxidant stress induces translocation of TLR4 to plasmalemmal lipid rafts. Moreover, the integrity of lipid rafts appears to be essential for this process.

Role of exocytosis in TLR4 translocation to the plasma membrane after oxidative stress

Exocytosis represents a general mechanism for delivery of molecules from cytoplasmic compartments to the plasma membrane. To study the role of exocytosis in TLR4 upregulation after oxidative stress, we applied two strategies to inhibit exocytosis. First, RAW 264.7 cells were exposed to jasplakinolide, a marine sponge toxin that induces excessive actin polymerization (25) and has been shown to physically interfere with exocytosis (26). Second, cytosolic Ca^{2+}, a requisite for exocytosis, was chelated by loading the cells

with 1,2-bis-(2-aminophenoxy)ethane-N,N,N',N'-tetraacetic acid tetra(acetoxymethyl) ester (BAPTA/AM) in a Ca^{2+}-free medium (27). To verify that these manipulations indeed abrogated exocytosis in cells, we tested the up-regulation of CD11b, which is known to be delivered to the cell surface through exocytosis. Fig. 7 (A and B) shows that both jasplakinolide and BAPTA prevented the H_2O_2- and LPS-induced CD11b up-regulation in RAW 264.7 cells. Next, we examined the effect of these strategies on oxidative stress–induced redistribution of TLR4. As shown in Fig. 7 (C and D), both jasplakinolide and calcium depletion prevented H_2O_2-stimulated increase in TLR4 surface level. Collectively, these findings suggest a role for exocytosis in the oxidant-induced increase in cell surface TLR4.

Effect of oxidant stress on the assembly of TLR4/MyD88 signaling molecules

Formation of a multi-molecular signaling complex containing cell surface TLR4 and adaptor molecules such as MyD88 is an important early step in LPS-induced signaling leading to downstream events, such as nuclear translocation of NF-κB (28). Having shown that oxidative stress induces movement of TLR4 to the plasma membrane, we examined whether oxidative stress might cause colocalization of MyD88 with TLR4 in a signaling complex, possibly in lipid rafts. Fig. 8 A shows that similar to TLR4, S/R also causes peripheralization of MyD88. Colocalization of Myd88 and TLR4 is indicated by the fluorescence overlay pictures. Further, inhibition of MyD88 peripheralization by NAC confirmed a role for oxidative stress in the effect (Fig. 8 A, right panels). The addition of H_2O_2 to RAW 264.7 cells also caused translocation of MyD88 to the membrane (Fig. 8 B). The specificity of the anti-MyD88 antibody was confirmed using a blocking peptide (Fig. 8 C). Next, recruitment of MyD88 into lipid rafts was examined. As shown in Fig. 8 D, MyD88 was detected in the raft fractions after H_2O_2 treatment, an effect that was prevented by cholesterol depletion before oxidative stress.

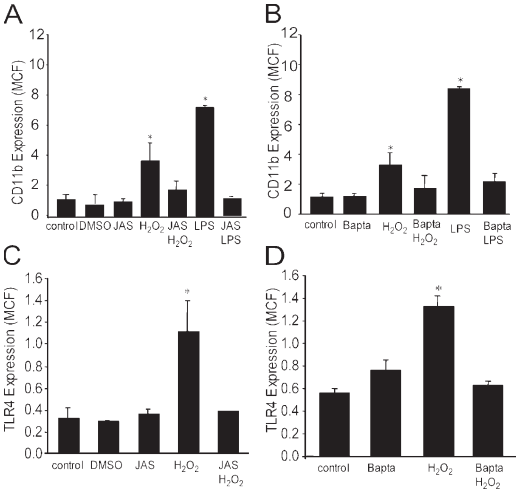

Figure 7. Role of exocytosis in TLR4 translocation to the plasma membrane after oxidant stress. Raw 264.7 cells remained untreated (control) or exposed to DMSO vehicle or 1 μM jaspakinolide (JAS) (A and C) for 30 min or 10 μM BAPTA/AM for 10 min (B and D). Cells were then exposed to 100 μM H_2O_2 for1 h or 0.1 μg/ml LPS for 30 min, followed by staining live with anti–CD11b-FITC (A and B) or anti-TLR4/MD2-FITC at 4°C (C and D). Fluorescence was analyzed by flow cytometry. Data are mean ± SEM of $n = 4$ per group. *, $P < 0.05$ for groups indicated versus all other groups without an asterisk.

The functional significance of lipid raft integrity in oxidative stress–induced macrophage priming

The LPS-induced aggregation of a signaling complex within lipid rafts appears to be a prerequisite for LPS-mediated NF-κB translocation in macrophages (21). We have shown that oxidative stress primed macrophages for earlier and increased responsiveness to subsequent LPS challenge (29). Therefore, we hypothesized that induction of assembly of the LPS receptor complex by oxidative stress might represent a mechanism for the priming of macrophages to subsequent challenge with LPS. We designed experiments to separate the role of TLR4 accumulation in lipid rafts in LPS signaling from the ability of oxidant stress to mobilize TLR4 to lipid rafts as a priming mechanism. In control studies, LPS caused a time-dependent

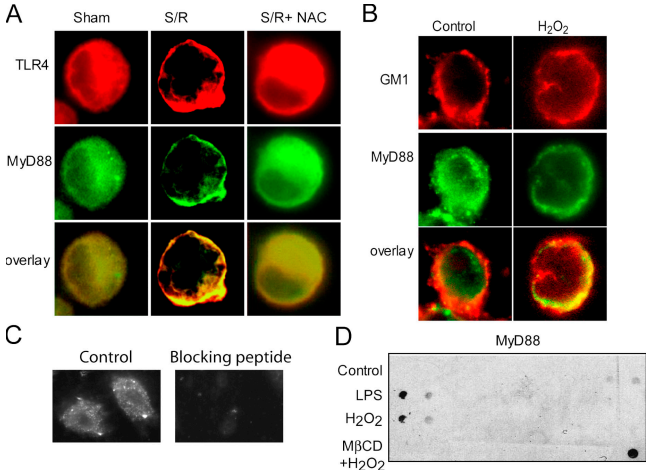

Figure 8. Oxidant stress induces colocalization of TLR4 and MyD88 in the plasma membrane. (A) Oxidant-dependent colocalization of TLR4 and MyD88 after S/R. AMs were stained with anti-TLR4 and anti-MyD88 primary as well as the corresponding secondary antibodies. Representative images ($n = 4$ experiments) are shown of TLR4 staining (red), MyD88 staining (green), or merged images. (B) Colocalization of GM1 and MyD88 after H_2O_2 treatment. RAW 264.7 cells, treated with 100 μM H_2O_2 for 1 h, were stained live at 4°C with rhodamine-CT_xB, fixed, permeabilized, and stained with anti-MyD88 antibody as in A. Representative images ($n = 3$ experiments) of GM1 staining (red), MyD88 staining (green), or merged image. (C) Specificity of the anti-Myd88 antibody. RAW 264.7 cells were immunostained as in A. In the right image, the primary antibody was added in the presence of a specific blocking peptide (D). RAW 264.7 cells were exposed to 0.1 μg/ml LPS or 100 μM H_2O_2. Where indicated, cells were pretreated with 10 mM MβCD. Lipid raft fractions were isolated and analyzed by dot blotting using MyD88 primary and horseradish peroxidase–coupled secondary antibody. Fractions 1–3 correspond to lipid rafts.

increase in NF-κB translocation with minimal translocation observed by 15 min and >80% of cells showing translocation by 30 min (Fig. 9 B). MβCD treatment caused an almost 40% drop in the cellular cholesterol content (Fig. 9 A) and prevented LPS-induced NF-κB translocation. Repletion of membrane cholesterol restored LPS responsiveness (Fig. 9, A and B). These studies established that cholesterol repletion after antecedent MβCD treatment permitted normal LPS signaling.

Consistent with our prior studies, Fig. 9 C shows that oxidative stress hastens NF-κB translocation in response to LPS, occurring by 15 min (17, 29). To test whether lipid raft integrity was required for this H_2O_2-induced priming, we treated cholesterol-depleted cells with H_2O_2, where TLR4 movement to lipid rafts was prevented. Next, we restored cholesterol levels to permit normal LPS signaling (as shown in Fig. 9 B). As illustrated in Fig. 9 C, MβCD treatment before H_2O_2 exposure followed by cholesterol repletion prevented the augmented p65 translocation by LPS observed in H_2O_2-treated cells at 15 min. Moreover, this was comparable to the effect of LPS alone added for 15 min. This was not due to toxicity or a nonspecific effect of MβCD because by 30 min, p65 translocation approximated that seen for the combined H_2O_2/LPS treatment. Importantly, cholesterol measurements showed that H_2O_2 treatment did not interfere with cholesterol repletion (Fig. 9 A). Moreover, cholesterol depletion does not interfere with H_2O_2-induced signaling (Fig. 4 D). Thus, inhibition of TLR4 cell surface translocation by MβCD appeared to prevent the primed macrophage phenotype. These experiments strongly suggest that lipid rafts are not only integral for LPS-mediated signaling but also critical for oxidant-induced macrophage priming for LPS responsiveness.

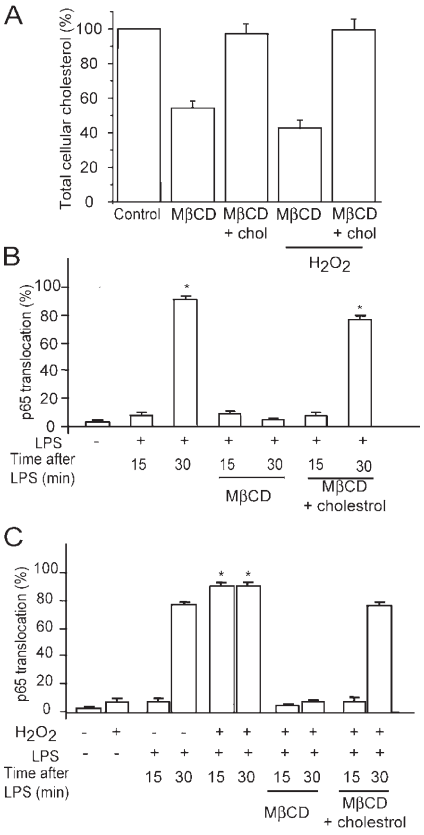

Figure 9. H_2O_2 treatment does not affect cholesterol depletion and repletion. (A) Cells were incubated with 10 mM MβCD for 30 min. Next, indicated samples were treated with 100 μM H_2O_2 for 1 h. Where indicated, cholesterol levels were restored using MβCD plus cholesterol. Total cellular cholesterol was measured. Data are normalized to control levels (100%). Data represent mean ± SE ($n = 3$ experiments). (B and C) Lipid raft integrity is required for oxidant-induced priming of LPS-stimulated NF-κB activation. (B) Cholesterol depletion inhibits and cholesterol repletion restores LPS-induced NF-κB nuclear translocation. RAW 264.7 cells were exposed to 0.1 μg/ml LPS for 15 or 30 min with or without cholesterol depletion. Where indicated, cholesterol levels were restored before the addition of LPS (MβCD+cholesterol). Cells were stained with anti-p65. NF-κB nuclear translocation was analyzed by fluorescence microscopy as described in Materials and methods. (C) Cholesterol depletion before H_2O_2 prevents LPS-induced early p65 translocation. Control or MβCD-treated cells were incubated with H_2O_2, followed by cholesterol repletion and addition of LPS where indicated. NF-κB nuclear translocation was analyzed as in A. Data are mean ± SEM of $n = 3$. *, $P < 0.05$ for groups indicated versus all other groups without an asterisk.

DISCUSSION

The clinical scenario of resuscitated hemorrhagic shock is known to render patients susceptible to the development of a systemic inflammatory response and organ dysfunction. Although several mechanisms undoubtedly contribute to this, the ability of antecedent S/R to prime inflammatory cells for increased responsiveness to a second stimulus, such as Gram-negative bacterial LPS, has provided a mechanistic framework for the investigation of post-resuscitation organ injury. These studies focus on the regulation of surface TLR4 expression after ischemia/reperfusion, a pathological process known to sensitize innate immune responses for enhanced LPS signaling both in vitro and in the in vivo setting (4, 5, 30). These experiments demonstrate that S/R, through the generation of oxidative stress, causes recruitment of TLR4 to the cell surface and that through the formation of these TLR4-containing receptor complexes, the cell becomes poised for increased responsiveness to LPS stimulation. These studies are the first to show that oxidative stress generated during ischemia/reperfusion alters subcellular TLR4 distribution in vivo, and thus they provide insights into the cellular mechanism whereby oxidative stress primes for enhanced LPS responsiveness.

Recent reports have suggested an important role for lipid rafts, detergent-insoluble cell membrane microdomains, in LPS signaling. Specifically, the clustering of TLR4/MD2 and other molecules, including CD14, heat shock proteins 70 and 90, the chemokine receptor CXCR4, and growth/differentiation factor 5, within lipid rafts and their confinement in these microdomains were determined as early steps in LPS signaling. Raft-disrupting agents, such as nystatin and MβCD, inhibited both enrichment of TLR4 in lipid rafts and LPS-stimulated downstream signaling via the MyD88/NF-κB

pathway (21). In these studies, we used both biochemical approaches and cell imaging techniques to demonstrate that oxidative stress generated by S/R in vivo or by H_2O_2 in vitro was able to induce migration of TLR4 into lipid rafts. Coupled with the immunofluorescence microscopy and the flow cytometry data demonstrating increased surface TLR4 expression after oxidative stress, these findings suggest movement of TLR4 from the cytoplasmic compartment to lipid rafts in the plasma membrane. Because lipid rafts are known to be present in various intracellular compartments, such as the Golgi apparatus or vesicles, it is possible that TLR4 may first move to one or more of these locations en route to the plasma membrane. It also appears that the integrity of the lipid raft microdomains is critical for TLR4 recruitment to the plasma membrane because disruption of these domains with MβCD prevented the oxidant-induced increase in TLR4 cell surface expression. This observation is also consistent with our finding that oxidant-induced exocytosis was involved in the translocation of TLR4 to the plasmalemma. Recent studies have reported that lipid rafts are involved in regulated exocytosis in various cells types based on the observation that cholesterol depletion prevents exocytosis (31). The mechanism of this raft-dependent exocytosis in part involves the clustering of SNARE proteins within raft domains. Conclusions regarding whether TLR4-containing vesicles translocate to the plasmalemmal rafts directly or migrate to the raft fraction after delivery to the plasma membrane will require further investigation.

The data suggest that mobilization of TLR4 into cell surface lipid rafts after oxidative stress plays an important role in the augmented cellular responsiveness to LPS stimulation. When oxidant-induced TLR4 mobilization to lipid rafts was prevented using the cholesterol-depleting agent MβCD, the increased responsiveness of the cells to LPS was prevented. One alternate explanation is that H_2O_2 might act through the activation of signaling cascades that are dependent on the integrity of lipid rafts, and thus its inability to prime after MβCD treatment may be due to an effect on H_2O_2-induced signaling. Data regarding p38 kinase activation by H_2O_2 with and without MβCD presented in Fig. 4 D demonstrate that MβCD does not globally inhibit H_2O_2-induced signaling. In addition, although these studies do not rule out every conceivable pathway, wherein H_2O_2 might have influenced LPS signaling in a raft-dependent manner, it does provide a clear relationship between oxidative stress, increased surface TLR4, involvement of lipid rafts in this TLR4 redistribution, and priming for LPS signaling. Recruitment of TLR4 to plasma membrane lipid rafts may have resulted in augmented signaling by several distinct mechanisms. First, the number of surface TLR4 molecules has been shown to generally correlate with LPS responsiveness. Overexpression of TLR4 in transgenic mice amplifies susceptibility to LPS treatment, both in vivo and in vitro (11). In these studies, there was a substantial increase in surface TLR4 expression after oxidative stress, potentially accounting for the enhanced NF-κB translocation after LPS treatment. Second, LPS-induced formation of the receptor complex within lipid rafts appears to be necessary to transduce the LPS signal. We propose that antecedent oxidant stress induces formation of the complex, even before exposure to LPS, such that the receptor complex is poised to respond rapidly when exposed to LPS. Although we did not measure the myriad of proteins known to localize in the LPS receptor complex, the adaptor protein MyD88, known to be enlisted to the complex during LPS signaling, was shown to colocalize with both TLR4 and the lipid raft fraction after oxidant exposure. Although early studies investigating an effect of oxidants on cellular activation clearly demonstrated that oxidative stress was able to induce NF-κB nuclear translocation (32), enrichment of TLR4 as well as MyD88 in lipid rafts in response to H_2O_2 treatment in these present studies was not sufficient to induce downstream signaling in the form of increased NF-κB translocation (Fig. 9 C), despite the fact that H_2O_2 was shown to activate other cell signaling pathways (Figs. 4 D and 7 A). This finding is likely due to the relatively low dose of H_2O_2 used in these studies and the early time course of observation for NF-κB. In our prior work, we showed that 100 μM H_2O_2 was able to induce a modest rise in NF-κB translocation at a delayed time point (1 h). This dose was chosen because it had been shown to be a priming dose for LPS stimulation in this system (17, 29). Similarly, the oxidant-dependent NF-κB translocation occurring in the lung after S/R is delayed and modest compared with LPS or the combination of shock plus LPS (5). This is consistent with the low-dose oxidant priming of AMs occurring in this setting and the effects on TLR4 redistribution seen in these studies. Besides the TLR4 redistribution per se, recent studies evaluating the responsiveness of cells to LPS and its analogues have also shown that the protein composition of the LPS receptor complex may vary depending on the stimulus and may influence downstream signaling (9). Oxidative stress may potentially induce an LPS receptor complex that diverts LPS signaling along an alternative pathway, leading to enhanced NF-κB translocation. In this regard, we recently reported that exposure of RAW 264.7 cells to H_2O_2 reprogrammed cells, such that LPS signaling was dependent on activation of src family kinases and involved the PI3-kinase/Akt pathway (17, 29). Src kinases are activated by oxidant stress (33) and move into lipid rafts to facilitate signaling (34). Further investigation evaluating the signaling pathways required for the oxidant-induced effects on TLR4 and the components of the oxidant-induced LPS receptor complex will provide insight into these possibilities.

The present studies demonstrate a marked change in TLR4 receptor density and distribution after oxidative stress, induced either by ischemia/reperfusion or by the addition of H_2O_2. In various other cell systems, oxidative stress may contribute to cell surface receptor density through altering the stability of newly synthesized protein in the endoplasmic reticulum, by inducing translocation of new proteins from the endoplasmic reticulum to the Golgi compartment and vesicular transport to the plasmalemma. With respect to the latter of these mechanisms, the glucose transporter GLUT4 is translocated

from cytoplasmic vesicles to the cell surface by oxidative stress (35). Ichimura et al. (36) demonstrated that oscillations in calcium levels induced production of reactive oxygen species, which in turn promoted exocytosis of P-selectin. In pancreatic acinar cells, reactive oxygen species generated by the hypoxanthine/xanthine oxidase system were able to induce increased exocytosis of amylase (37). Consistent with this mechanism, two distinct strategies aimed at preventing exocytosis of CD11b-containing intracellular vesicular compartments in macrophages also precluded oxidant-induced up-regulation of TLR4. Specifically, polymerization of the actin cytoskeleton with jasplakinolide and calcium depletion inhibited translocation of TLR4 to the cell surface by H_2O_2. These and other studies suggest that the effect of oxidative stress on exocytosis may involve alterations in intracellular calcium levels.

The precise intracellular source of TLR4 requires further elucidation. Espevik et al. (38) recently showed that in an epithelial cell line, entire lipid raft fractions containing TLR4, CD14, and MD-2 continuously and rapidly recycle between the Golgi complex and the plasma membrane. In human monocytes, localization of TLR4 to perinuclear compartments was suggested to be evidence of its presence in the Golgi, although no formal localization studies have been performed (39). In RAW 264.7 cells as well as in rat AMs, the intracellular localization of TLR4 appears more diffuse, consistent with its presence in preformed vesicles. Further definition of the cytoplasmic localization of TLR4 in the cells of monocyte/macrophage lineage should provide insight into the preferred approaches to studying the mechanisms whereby oxidative stress induces an increase in surface TLR4 expression.

Alterations in the redox status of cells have been shown to affect a multitude of signaling pathways (40). With respect to LPS signaling, these present experiments provide evidence that oxidative stress generated during ischemia/reperfusion may exert its effects by regulating the distribution of the most proximal component of the signaling cascade, namely the LPS receptor complex. Future studies defining the mechanism of oxidant-induced TLR4 redistribution may provide fundamental insights into the regulation of TLR4 in monocytes/macrophages and suggest novel therapeutic approaches in disease states wherein the process of ischemia/reperfusion contributes to the pathogenesis of disease.

MATERIALS AND METHODS

Animal model. The animal protocol was approved by the Animal Care Committee of St. Michael's Hospital (protocol no. ACC756). S/R was performed as described previously (14). In brief, male Sprague-Dawley rats were anaesthetized, and the right carotid artery was cannulated for monitoring of mean arterial pressure, blood sampling, and resuscitation. Mean arterial pressure was reduced to 40 mmHg by blood withdrawal and maintained between 35 and 45 mmHg by additional blood withdrawal or infusion of Ringer's lactate (Baxter Co.) if necessary. Shed blood was collected into 0.1 ml sodium citrate/ml blood. After 60 min, animals were resuscitated with their shed blood and an equivalent amount of Ringer's lactate with or without 0.5 g/kg NAC (Mucomyst; Shire, Inc.) or 10 mg/kg Trolox over a 2-h period. Animals were killed by a pentobarbital (MTC Pharmaceuticals) overdose, and AMs were recovered by bronchoalveolar lavage with cold PBS (Invitrogen), followed by centrifugation at 300 *g* (10 min).

Cell culture and activation. The murine macrophage cell line, RAW 264.7 (American Type Culture Collection), was cultured at 37°C in a humidified atmosphere of 5% CO_2 in endotoxin-free DMEM (Invitrogen) with 100 U/ml penicillin, 100 μg/ml streptomycin (Invitrogen), and 10% FCS (Hyclone Lab, Inc.). Experiments were performed in HBSS (Invitrogen) supplemented with 2% FCS. The following treatments were applied: 100 μM (or the indicated concentration) H_2O_2, 0.1 μg/ml LPS (*Escherichia coli* O111:B4; Sigma-Aldrich), 0.1 mM xanthine and 3 U/ml xanthine oxide, and 50 μM menadione. In the functional studies, cells were exposed to H_2O_2 for 1 h, followed by LPS for 15–60 min. Where indicated, cells were treated with 10 μM BAPTA/AM (Calbiochem) for 10 min or 1 μM jasplakinolide (Invitrogen) for 30 min at 37°C before adding oxidants. Reactions were stopped by placing cells on ice.

Immunofluorescence microscopy. AMs or RAW264.7 cells on coverslips were fixed with 4% paraformaldehyde (Canemco-MARivac) for 30 min, permeabilized with 0.2% Triton X-100 in PBS for 20 min, blocked with 5% bovine serum albumin for 1 h, and incubated with the indicated antibody. The following primary antibodies were used: anti-TLR4 antibody (H-80; 1:200; for rat AMs), anti-MyD88 (F-19; 1:200), and anti-p65 (1:50) from Santa Cruz Biotechnology, Inc.; and FITC-conjugated anti-TLR4/MD2 (MTS510; for RAW 264.7 cells) from StressGen Biotechnologies. The two anti-TLR4 antibodies differ insofar as the H-80 antibody recognizes TLR4, whereas the MTS510 recognizes the MD-2/TLR4 complex. FITC- or Cy3-conjugated Fab fragment secondary antibodies were from Jackson ImmunoResearch Laboratories, and Alexa 488–labeled anti–goat antibody was from Invitrogen. GM-1 ganglioside, a component of lipid rafts, was detected by incubating live cells with rhodamine (TRITC)-conjugated CT_xB (1:500; List Biological Laboratories) before fixation. The coverslips were mounted using DAKO medium (DakoCytomation) and visualized with a Nikon TE200 fluorescence microscope (100× objective) coupled to an Orca 100 camera (Hamamatsu Photonics) driven by Simple PCI software (Compix Inc.). Where indicated, a Zeiss LSM 510 confocal microscope with a 100× objective was used to acquire 0.5-μm-thick serial optical slices. Images of representative focal planes are shown. Image analysis was performed using the Scionimage software. Peripheralization was defined as a ≥80% increase in the ratio of fluorescence intensities at the cell periphery and the cytosol (at 0.5 μm distance from the membrane). The percentage of cells with peripheralized TLR4 under various conditions was calculated by scoring 100 cells. NF-κB translocation was analyzed as described previously (17). The percentage of cells with nuclear p65 staining was determined by counting an average of 100 cells for each group. During quantitation, the observer was blinded to the experimental group.

Flow cytometry. Cell surface expression of TLR4 and CD11b was detected by flow cytometry of live cells stained with anti-TLR4 (H-80), anti-TLR4/MD2 (MTS510), or anti-CD11b/CD18 (Mac-1; Cedarlane Laboratories) and the corresponding FITC-labeled secondary antibody where required. 10,000 cells/condition were analyzed in a FACScan (Becton Dickinson) using FL1 525 mM Band Pass detector at an excitation wavelength of 488 nm. Results were expressed as mean channel fluorescence.

FRET. For FRET experiments, live RAW264.7 cells were stained at 4°C with anti-TLR4 antibody (H-80) followed by an FITC-conjugated anti–rabbit Fab fragment and rhodamine-CT_xB. The fluorescence was determined at 37°C using a DeltaRAM illumination system from Photon Technologies, Inc. operated by FELIX software. The excitation wavelength was 480 ± 5 nm and emission was detected at 510 ± 10 nm (green emission) and at >590 nm (red emission) for at least six cells/coverslip. For each condition, at least 20 cells from three to four coverslips were measured.

Manipulation and measurement of cellular cholesterol. Cholesterol was depleted and repleted in RAW264.7 cells using a modified procedure of

Furuchi et al. (41) and Roy et al. (42). In brief, cells were treated with 10 mM MβCD for 30 min at 37°C in HBSS. Cholesterol repletion was then achieved by incubation with 80 μg/ml cholesterol and 0.2% MβCD for 30 min at 37°C. The total cholesterol content was determined using the Amplex red cholesterol assay kit from Invitrogen.

Isolation and detection of lipid rafts. Lipid rafts were isolated as described previously (24). RAW264.7 cells (2×10^7 cells/ml) were lysed in 0.25 ml TKM buffer (50 mM Tris, pH 7.4, 25 mM KCl, 5 mM $MgCl_2$, and 1 mM EDTA) containing 0.5% wt/vol Brij58 (Sigma-Aldrich) and protease inhibitors (Roche Diagnostics) on ice for 30 min. Lysates was mixed with an equal volume cold 80% wt/vol sucrose in TKM and overlaid with 4.3 ml cold 36% sucrose, followed by 0.2 ml 5% sucrose. The gradients were subjected to ultracentrifugation at 200 000 *g* at 4°C for 18 h. Fractions were collected from the top of the gradient. An equal volume of each fraction was diluted in 10 μl TBS-T buffer (20 mM Tris, pH 7.4, 150 mM NaCl, and 0.05% Tween 20) containing 0.1% Triton X-100 and loaded onto Protran Nitrocellulose Sheet (0.45-μm pore; S&S BioScience) using Dot Blot (Bio-Rad Laboratories). The membrane was blocked in 5% milk in TBS-T, followed by incubation with CT_xB–horseradish peroxidase (1:500; List Biological Laboratories), anti-TLR4 (H-80), or anti-MyD88 (F-19) for 1 h. Where required, horseradish peroxidase–conjugated secondary antibody (1:3,000 dilution for 1 h) was used. Labeling was visualized using enhanced chemiluminescence (PerkinElmer).

Western blotting. Proteins were detected using Western blotting as described previously (43). Protein concentration was determined using the Bradford protein assay (Bio-Rad Laboratories). Equal loading was verified using Ponceau S staining of the membranes. The phospho-p38 antibody was from Cell Signaling.

Statistical analysis. Data are presented as mean ± standard error of *n* determinations as indicated in the figure legends. Data were analyzed by one-way analysis of variance, and post hoc testing was performed using the Bonferroni modification of the *t* test with significance at $P < 0.05$. Blots and images shown are representatives of at least three separate determinations.

The authors acknowledge the help of Dr. Michael Julius in lipid raft separation and detection.

This work was supported by the Canadian Institutes of Health Research. K.A. Powers is a recipient of awards from the American College of Surgeons and the Canadian Association For Clinical Microbiology and Infectious Diseases. R.G. Khadaroo is supported by the Alberta Heritage Foundation. A. Kapus and K. Szászi are recipients of support awards from the Canadian Institutes of Health Research.

The authors have no conflicting financial interests.

Submitted: 2 May 2006
Accepted: 19 June 2006

REFERENCES

1. Sauaia, A., F.A. Moore, E.E. Moore, and D.C. Lezotte. 1996. Early risk factors for postinjury multiple organ failure. *World J. Surg.* 20:392–400.
2. Regel, G., M. Grotz, T. Weltner, J.A. Sturm, and H. Tscherne. 1996. Pattern of organ failure following severe trauma. *World J. Surg.* 20:422–429.
3. Botha, A.J., F.A. Moore, E.E. Moore, F.J. Kim, A. Banerjee, and V.M. Peterson. 1995. Postinjury neutrophil priming and activation: an early vulnerable window. *Surgery.* 118:358–364.
4. Moore, F.A., and E.E. Moore. 1995. Evolving concepts in the pathogenesis of postinjury multiple organ failure. *Surg. Clin. North Am.* 75:257–277.
5. Fan, J., J.C. Marshall, M. Jimenez, P.N. Shek, J. Zagorski, and O.D. Rotstein. 1998. Hemorrhagic shock primes for increased expression of cytokine-induced neutrophil chemoattractant in the lung: role in pulmonary inflammation following lipopolysaccharide. *J. Immunol.* 161:440–447.
6. Fan, J., A. Kapus, Y.H. Li, S. Rizoli, J.C. Marshall, and O.D. Rotstein. 2000. Priming for enhanced alveolar fibrin deposition after hemorrhagic shock: role of tumor necrosis factor. *Am. J. Respir. Cell Mol. Biol.* 22:412–421.
7. Takeda, K., and S. Akira. 2004. TLR signaling pathways. *Semin. Immunol.* 16:3–9.
8. Triantafilou, M., and K. Triantafilou. 2004. Heat-shock protein 70 and heat-shock protein 90 associate with Toll-like receptor 4 in response to bacterial lipopolysaccharide. *Biochem. Soc. Trans.* 32:636–639.
9. Triantafilou, M., K. Brandenburg, S. Kusumoto, K. Fukase, A. Mackie, U. Seydel, and K. Triantafilou. 2004. Combinational clustering of receptors following stimulation by bacterial products determines lipopolysaccharide responses. *Biochem. J.* 381:527–536.
10. Poltorak, A., X. He, I. Smirnova, M.Y. Liu, C. Van Huffel, X. Du, D. Birdwell, E. Alejos, M. Silva, C. Galanos, et al. 1998. Defective LPS signaling in C3H/HeJ and C57BL/10ScCr mice: mutations in Tlr4 gene. *Science.* 282:2085–2088.
11. Bihl, F., L. Salez, M. Beaubier, D. Torres, L. Lariviere, L. Laroche, A. Benedetto, D. Martel, J.M. Lapointe, B. Ryffel, and D. Malo. 2003. Overexpression of Toll-like receptor 4 amplifies the host response to lipopolysaccharide and provides a survival advantage in transgenic mice. *J. Immunol.* 170:6141–6150.
12. Kalis, C., B. Kanzler, A. Lembo, A. Poltorak, C. Galanos, and M.A. Freudenberg. 2003. Toll-like receptor 4 expression levels determine the degree of LPS-susceptibility in mice. *Eur. J. Immunol.* 33:798–805.
13. Nomura, F., S. Akashi, Y. Sakao, S. Sato, T. Kawai, M. Matsumoto, K. Nakanishi, M. Kimoto, K. Miyake, K. Takeda, and S. Akira. 2000. Cutting edge: endotoxin tolerance in mouse peritoneal macrophages correlates with down-regulation of surface toll-like receptor 4 expression. *J. Immunol.* 164:3476–3479.
14. Fan, J., A. Kapus, P.A. Marsden, Y.H. Li, G. Oreopoulos, J.C. Marshall, S. Frantz, R.A. Kelly, R. Medzhitov, and O.D. Rotstein. 2002. Regulation of Toll-like receptor 4 expression in the lung following hemorrhagic shock and lipopolysaccharide. *J. Immunol.* 168:5252–5259.
15. Powers, K.A., A. Kapus, R.G. Khadaroo, R. He, J.C. Marshall, T.F. Lindsay, and O.D. Rotstein. 2003. Twenty-five percent albumin prevents lung injury following shock/resuscitation. *Crit. Care Med.* 31:2355–2363.
16. Khadaroo, R.G., R. He, J. Parodo, K.A. Powers, J.C. Marshall, A. Kapus, and O.D. Rotstein. 2004. The role of the Src family of tyrosine kinases after oxidant-induced lung injury in vivo. *Surgery.* 136:483–488.
17. Khadaroo, R.G., A. Kapus, K.A. Powers, M.I. Cybulsky, J.C. Marshall, and O.D. Rotstein. 2003. Oxidative stress reprograms lipopolysaccharide signaling via Src kinase-dependent pathway in RAW 264.7 macrophage cell line. *J. Biol. Chem.* 278:47834–47841.
18. Lai, E.C. 2003. Lipid rafts make for slippery platforms. *J. Cell Biol.* 162:365–370.
19. Jiang, Q., S. Akashi, K. Miyake, and H.R. Petty. 2000. Lipopolysaccharide induces physical proximity between CD14 and toll-like receptor 4 (TLR4) prior to nuclear translocation of NF-kappa B. *J. Immunol.* 165: 3541–3544.
20. Triantafilou, M., and K. Triantafilou. 2002. Lipopolysaccharide recognition: CD14, TLRs and the LPS-activation cluster. *Trends Immunol.* 23:301–304.
21. Triantafilou, M., K. Miyake, D.T. Golenbock, and K. Triantafilou. 2002. Mediators of innate immune recognition of bacteria concentrate in lipid rafts and facilitate lipopolysaccharide-induced cell activation. *J. Cell Sci.* 115:2603–2611.
22. Pfeiffer, A., A. Bottcher, E. Orso, M. Kapinsky, P. Nagy, A. Bodnar, I. Spreitzer, G. Liebisch, W. Drobnik, K. Gempel, et al. 2001. Lipopolysaccharide and ceramide docking to CD14 provokes ligand-specific receptor clustering in rafts. *Eur. J. Immunol.* 31:3153–3164.
23. Niu, S.L., D.C. Mitchell, and B.J. Litman. 2002. Manipulation of cholesterol levels in rod disk membranes by methyl-beta-cyclodextrin: effects on receptor activation. *J. Biol. Chem.* 277:20139–20145.
24. Marmor, M.D., and M. Julius. 2001. Role for lipid rafts in regulating interleukin-2 receptor signaling. *Blood.* 98:1489–1497.
25. Holzinger, A. 2001. Jasplakinolide. An actin-specific reagent that promotes actin polymerization. *Methods Mol. Biol.* 161:109–120.
26. Rizoli, S.B., A. Kapus, J. Parodo, J. Fan, and O.D. Rotstein. 1999. Hypertonic immunomodulation is reversible and accompanied by changes in CD11b expression. *J. Surg. Res.* 83:130–135.

27. Collatz, M.B., R. Rudel, and H. Brinkmeier. 1997. Intracellular calcium chelator BAPTA protects cells against toxic calcium overload but also alters physiological calcium responses. *Cell Calcium*. 21:453–459.
28. Suzuki, N., S. Suzuki, G.S. Duncan, D.G. Millar, T. Wada, C. Mirtsos, H. Takada, A. Wakeham, A. Itie, S. Li, et al. 2002. Severe impairment of interleukin-1 and Toll-like receptor signalling in mice lacking IRAK-4. *Nature*. 416:750–756.
29. Khadaroo, R.G., J. Parodo, K.A. Powers, G. Papia, J.C. Marshall, A. Kapus, and O.D. Rotstein. 2003. Oxidant-induced priming of the macrophage involves activation of p38 mitogen-activated protein kinase through an Src-dependent pathway. *Surgery*. 134:242–246.
30. Waxman, K. 1996. Shock: ischemia, reperfusion, and inflammation. *New Horiz*. 4:153–160.
31. Salaun, C., D.J. James, and L.H. Chamberlain. 2004. Lipid rafts and the regulation of exocytosis. *Traffic*. 5:255–264.
32. Schreck, R., P. Rieber, and P.A. Baeuerle. 1991. Reactive oxygen intermediates as apparently widely used messengers in the activation of the NF-kappa B transcription factor and HIV-1. *EMBO J*. 10:2247–2258.
33. Abe, J., M. Takahashi, M. Ishida, J.D. Lee, and B.C. Berk. 1997. c-Src is required for oxidative stress-mediated activation of big mitogen-activated protein kinase 1. *J. Biol. Chem*. 272:20389–20394.
34. Hoessli, D.C., S. Ilangumaran, A. Soltermann, P.J. Robinson, B. Borisch, and D. Nasir Ud. 2000. Signaling through sphingolipid microdomains of the plasma membrane: the concept of signaling platform. *Glycoconj. J*. 17:191–197.
35. Akhand, A.A., J. Du, W. Liu, K. Hossain, T. Miyata, F. Nagase, M. Kato, H. Suzuki, and I. Nakashima. 2002. Redox-linked cell surface-oriented signaling for T-cell death. *Antioxid. Redox Signal*. 4:445–454.
36. Ichimura, H., K. Parthasarathi, S. Quadri, A.C. Issekutz, and J. Bhattacharya. 2003. Mechano-oxidative coupling by mitochondria induces proinflammatory responses in lung venular capillaries. *J. Clin. Invest*. 111:691–699.
37. Rosado, J.A., A. Gonzalez, G.M. Salido, and J.A. Pariente. 2002. Effects of reactive oxygen species on actin filament polymerisation and amylase secretion in mouse pancreatic acinar cells. *Cell. Signal*. 14:547–556.
38. Espevik, T., E. Latz, E. Lien, B. Monks, and D.T. Golenbock. 2003. Cell distributions and functions of Toll-like receptor 4 studied by fluorescent gene constructs. *Scand. J. Infect. Dis*. 35:660–664.
39. Latz, E., A. Visintin, E. Lien, K.A. Fitzgerald, B.G. Monks, E.A. Kurt-Jones, D.T. Golenbock, and T. Espevik. 2002. Lipopolysaccharide rapidly traffics to and from the Golgi apparatus with the toll-like receptor 4-MD-2-CD14 complex in a process that is distinct from the initiation of signal transduction. *J. Biol. Chem*. 277:47834–47843.
40. Poli, G., G. Leonarduzzi, F. Biasi, and E. Chiarpotto. 2004. Oxidative stress and cell signalling. *Curr. Med. Chem*. 11:1163–1182.
41. Furuchi, T., and R.G. Anderson. 1998. Cholesterol depletion of caveolae causes hyperactivation of extracellular signal-related kinase (ERK). *J. Biol. Chem*. 273:21099–21104.
42. Roy, S., R. Luetterforst, A. Harding, A. Apolloni, M. Etheridge, E. Stang, B. Rolls, J.F. Hancock, and R.G. Parton. 1999. Dominant-negative caveolin inhibits H-Ras function by disrupting cholesterol-rich plasma membrane domains. *Nat. Cell Biol*. 1:98–105.
43. Szaszi, K., J.J. Jones, A.B. Nathens, A.Y. Lo, P.A. Marsden, A. Kapus, and O.D. Rotstein. 2005. Glutathione depletion inhibits lipopolysaccharide-induced intercellular adhesion molecule 1 synthesis. *Free Radic. Biol. Med*. 38:1333–1343.